The Journal of Immunology

The NKG2D Ligand ULBP2 Is Specifically Regulated through an Invariant Chain–Dependent Endosomal Pathway

Franziska Uhlenbrock, Michael Hagemann-Jensen, Stephanie Kehlet, Lars Andresen, Silvia Pastorekova and Søren Skov

J Immunol 2014; 193:1654-1665; Prepublished online 14 July 2014;
doi: 10.4049/jimmunol.1303275
http://www.jimmunol.org/content/193/4/1654

The Journal of Immunology is published twice each month by
The American Association of Immunologists, Inc.,
1451 Rockville Pike, Suite 650, Rockville, MD 20852

Print ISSN: 0022-1767 Online ISSN: 1550-6606.

The NKG2D Ligand ULBP2 Is Specifically Regulated through an Invariant Chain–Dependent Endosomal Pathway

Franziska Uhlenbrock,*[,1] Michael Hagemann-Jensen,*[,1] Stephanie Kehlet,* Lars Andresen,* Silvia Pastorekova,[†] and Søren Skov*

Soluble ULBP2 is a marker for poor prognosis in several types of cancer. In this study we demonstrate that both soluble and cell surface–bound ULBP2 is transported via a so far unrecognized endosomal pathway. ULBP2 surface expression, but not MICA/B, could specifically be targeted and retained by affecting endosomal/lysosomal integrity and protein kinase C activity. The invariant chain was further essential for endosomal transport of ULBP2. This novel pathway was identified through screening experiments by which methylselenic acid was found to possess notable NKG2D ligand regulatory properties. The protein kinase C inhibitor methylselenic acid induced MICA/B surface expression but dominantly blocked ULBP2 surface transport. Remarkably, by targeting this novel pathway we could specifically block the production of soluble ULBP2 from different, primary melanomas. Our findings strongly suggest that the endosomal transport pathway constitutes a novel therapeutic target for ULBP2-producing tumors. ***The Journal of Immunology*****, 2014, 193: 1654–1665.**

Transformed, infected, or stressed cells can alert the immune system through the surface expression of NKG2D ligands. The malfunctioning cells are then recognized and targeted by NKG2D-expressing immune effector cells. The number of different escape mechanisms used by viruses and neotransformed cells to avoid this form of immune recognition highlights the importance of the NKG2D system. The activating NKG2D receptor is expressed on NK cells, NKT cells, $CD8^+$ T cells, γδ T cells, and some activated $CD4^+$ T cells (1–4). The NKG2D ligands are nonclassical MHC class I–like molecules (1) and are not significantly expressed on healthy human cells. Several NKG2D ligands exist that primarily belong to the polymorphic *MIC* (*MICA* and *MICB*) or *RAET1* (*ULBP1–6*) gene families (5).

Defects in the regulation of NKG2D ligand surface expression are associated with diseases ranging from autoimmunity to cancer. Excessive expression of NKG2D ligands is characteristic of various autoimmune diseases (2), whereas reduced ligand expression due to intracellular retention or cell surface cleavage can be observed in cancers and virus-infected cells (6–9). The importance of NKG2D ligands has resulted in an emerging interest in their regulation (10–13), with a recent focus on posttranslational regulation of NKG2D ligands (14–18). Many tumors evade immunity by shedding or exosomal release of NKG2D ligands (19–21). The reduced NKG2D ligand surface expression renders the tumor cells undetectable by the NKG2D immune effector cells. Soluble NKG2D ligands also interact and subsequently downregulate the expression of NKG2D on NK and CD8 T cells (7). The production of soluble NKG2D ligands has been described in melanoma, prostate and ovarian cancers, as well as B cell chronic lymphocytic leukemia (B-CLL) (19, 22–24). Soluble ULBP2 is in particular associated with a poor prognosis and was identified as an independent predictive factor for poor treatment-free survival (19).

MHC class II molecules are transported from the endoplasmic reticulum (ER) to the cell surface through the endosomal/lysosomal compartment (25). Protein kinase C (PKC) activity is important for endosomal transport, particularly endosomal/lysosomal transport and exocytosis (26, 27) and trafficking to the MHC class II compartments, and Ag presentation is critically dependent on PKC activity (28–30). MHC class II transport from the ER to endosomes is facilitated by the invariant chain, which possesses an endosomal targeting motif (31). MHC class I molecules normally present intracellular proteasome-digested peptides through a conventional ER/Golgi cell surface pathway (25). Certain MHC class I homologous molecules such as CD1a and MR1 are, however, transported to the cell surface through a mechanism similar to MHC class II molecules (32, 33). Notably, CD1d and MR1 associate with Ii to ensure endosomal trafficking and surface transport (32, 34). PKC activity is further important for CD1d surface expression and Ag presentation (35).

In this study, we found that ULBP2 is transported to the cell surface via an endosomal pathway. The alternative transport pathway emphasizes the diverse regulation of NKG2D ligands that limits the ability of pathogens to broadly obstruct the different NKG2D ligands. Certain tumors, such as melanomas, however, exploit this novel pathway to secrete large amounts of soluble ULBP2 to escape immune recognition.

Materials and Methods

Cell lines

Two Jurkat T cell lines were used in this study: Jurkat E6-1 was purchased from the American Type Culture Collection, and Jurkat Tag-9 was provided

*Section for Experimental Animal Models, Laboratory of Immunology, Faculty of Health and Medical Sciences, University of Copenhagen, DK-1870 Frederiksberg, Denmark; and [†]Department of Molecular Medicine, Institute of Virology, Slovak Academy of Sciences, 845 05 Bratislava, Slovak Republic

[1]F.U. and M.H.-J. contributed equally to this work.

Received for publication December 9, 2013. Accepted for publication June 9, 2014.

This work was supported by European Union Marie Curie Initial Training Networks Biomedical Engineering for Cancer and Brain Disease Diagnosis and Therapy Development Grant PITN-GA-2010-264417, as well as by Danish Council for Independent Research/Medical Sciences Grant DFF-1331-00169.

Address correspondence and reprint requests to Prof. Søren Skov, University of Copenhagen, Laboratory of Immunology, Stigbøjlen 7, DK-1870 Frederiksberg, Denmark. E-mail address: sosk@sund.ku.dk

Abbreviations used in this article: B-CLL, B cell chronic lymphocytic leukemia; ER, endoplasmic reticulum; h, human; MSA, methylselenic acid; PKC, protein kinase C; RPLP0, ribosomal protein, large, P0; SAHA, suberoylanilide hydroxamic acid; siRNA, small interfering RNA.

www.jimmunol.org/cgi/doi/10.4049/jimmunol.1303275

by Dr. Carsten Geisler (Department of International Health, Immunology and Microbiology, University of Copenhagen, Copenhagen, Denmark). Jurkat Tag-9 cells are stably transfected with the large T Ag from SV40, and they were primarily used for transient transfection studies. The PC3 cell line was also purchased from the American Type Culture Collection. The HEK293T cell line was provided by Novo Nordisk (Malov, Denmark). The melanoma cell lines FM-78, FM-86, and SK-Mel28 were provided by Dr. Per thor Straten (Center for Cancer Immune Therapy, Herlev University Hospital, Herlev, Denmark). The cell line U373 was provided by Dr. Amy Hudson (Medical College of Wisconsin, Milwaukee, WI). With the exception of HEK293T and U373 cells, all cell lines were grown in 10% FBS/RPMI 1640 (Sigma-Aldrich) supplemented with 2 mM glutamine and 2 mM penicillin and streptomycin. HEK293T and U373 cells were grown in 10% DMEM plus GlutaMAX with 2 mM penicillin and streptomycin.

Reagents

FR901228 was provided by the National Cancer Institute (Bethesda, MD). Trichostatin A and suberoylanilide hydroxamic acid (SAHA) were from Alexis Biochemicals. Methylselenic acid (MSA), TCA, sodium butyrate, PMA, ammonium chloride, and chloroquine diphosphate salt were from Sigma-Aldrich. Gö 6983 and Gö 6976 were from Tocris Bioscience. TRIzol reagent was from Invitrogen. Bafilomycin A1, ingenol, and ingenol-3-angelate were from LC Laboratories.

Isolation and activation of human blood cells

PBMCs were isolated by Ficoll separation from buffy coats obtained from healthy blood donors (Blood Bank, Copenhagen University Hospital, Copenhagen, Denmark) and cultured in RPMI 1640 supplemented with 10% human serum (Lonza), 2 mM glutamine, and 2 mM penicillin and streptomycin. For generation of long-term–stimulated plus restimulated T cells, PBLs were activated using CD3/CD28 beads according to the manufacturer's instructions. After 3 d, cells were supplied with extra RPMI 1640 containing 30 U/ml IL-2 (PeproTech). After 10–12 d of incubation, cells were restimulated using CD3/CD28 beads for 3 d. The beads were then removed and the cells were treated with FR901228 and MSA and analyzed by flow cytometry. For monocyte isolation by plastic adherence, 10×10^6 PBMCs per well were distributed into six-well plates and allowed to adhere at 37°C for 1 h in 2 ml 10% human serum (Lonza)/RPMI 1640 with 2 mM glutamine, penicillin, and streptomycin. Nonadherent cells were removed and the adherent cells were cultured in 2 ml RPMI 1640 containing either 0.5 or 5 ng/ml IFN-γ (R&D Systems). Monocytes were treated with 10 μM MSA and analyzed by flow cytometry.

NKG2D downmodulation assay

From purified PBLs, CD4 T cells were removed using a Dynal $CD4^+$ isolation kit. CD4-depleted PBLs were stimulated with IL-15 (PeproTech) for 3 d. Afterward, PBLs were cocultured with pretreated Jurkat E6-1 cells (with or without FR901228 or MSA) for 1–2 h at different E:T ratios. The blocking of NKG2D ligands was achieved by preincubating the Jurkat E6-1 effector cells (with or without MSA) for 30 min at 4°C with hNKG2D-Fc (R&D Systems, 1299-NK) at a final concentration of 2 μg/ml.

Plasmids and promoter constructs

The MICA promoter plasmid p3.2k-WT-GFP and the +2 control plasmid were previously described (27). Promoter activity was calculated by multiplying the percentage of GFP-expressing cells with the mean fluorescence intensity of these cells. The invariant chain construct (Ii31/33) was provided by Dr. Norbert Koch (University of Bonn, Bonn, Germany) (36). The GFP-ULBP2 plasmid was generated using phosphorothioate-based, ligase-independent gene cloning (37). We produced two PCR products using PfuUltra II Fusion HS DNA polymerase (Stratagene): a 681-bp ULBP2 PCR product using the ULBP2-FLAG plasmid as template, and a 6332-bp GFP-Myc PCR product using the GFP-MICA*018 plasmid as template. PCR products were treated with iodine to create an overhang. Finally, cleaved ULBP2 and GFP-Myc PCR products were hybridized. The following phosphorothioate primers (Eurofins MWG Operon) were used (lowercase characters indicate phosphoro-tailed bases): PTO-ULBP2, forward, 5′-agctggtgcaGGCTGGTCCCGGGCTGGGCGAGCCGA-3′, reverse, 5′-gccctctagaTCAGATGCCAGGGAGGATGAAGCAGGGGAGGAT-3; PTO-GFP-Myc, forward, 5′-tctagagggcCCTATTCTATAGTGTCACCTAAATGCTAG-3′, reverse, 5′-tgcaccagctCCCTCGAGGTCCTCTTCAGAG-3′. The construct was sequenced (Eurofins MWG Operon) to verify the correct orientation and sequence of the insert.

Transient transfections

Transient transfections of Jurkat Tag-9 and FM-86 cell lines were performed using the Amaxa Nucleofector device (Lonza) according to the manufacturer's protocol. In short, for the Jurkat Tag-9 cell line $1.5–3 \times 10^6$ cells were resuspended in 100 μl Ingenio electroporation solution (Mirus Bio), mixed with 1 μg plasmid/1×10^6 cells, and pulsed using the Nucleofector program G-010. For silencing experiments, 1×10^6 cells were transfected with different small interfering RNAs (siRNAs) targeting the Ii. The following siRNAs were used: endoribonuclease-prepared siRNA (human) CD74/Ii (Sigma-Aldrich, EHU157961) and CD74/Ii (human) siRNA (Santa Cruz Biotechnology, sc-35023). For the FM-86 cell line, 2.5×10^6 cells were resuspended in 100 μl Nucleofector solution T (Lonza), mixed with 1 μg plasmid/1×10^6 cells, and pulsed using the Nucleofector program U-020. The expression of the plasmids was measured after 18–48 h.

Quantitative real-time PCR

RNA was isolated from 1×10^6 Jurkat E6-1 cells using TRIzol reagent and reverse-transcribed using SuperScript III reverse transcriptase enzyme according to the manufacturer's protocol. PCR was performed using standard conditions. MICA primer sequences were: MICA_523, forward, 5′-GCCATGAACGTCAGGAATTT-3′; MICA_760, reverse, 5′-GACGCCAGCTCAGTGTGATA-3′. ULBP2 primer sequences were: ULBP2_378, forward, 5′-CAGAGCAACTGCGTGACATT-3′; ULBP2_610, reverse, 5′-GGCCACAACCTTGTCATTCT-3′. The housekeeping gene ribosomal protein, large, P0 (RPLP0) was used as a normalization control. RPLP0 primer sequences were: RPLP0, forward 5′-GCTTCCTGGAGGGTGTCC-3′, reverse, 5′-GGACTCGTTTGTACCCGTTG-3′. All primers were purchased from Eurofins MWG Operon. Quantitative real-time PCR was performed using the Brilliant II SYBR Green qPCR Master Mix kit with low ROX (Stratagene). The real-time PCR reactions were performed on a Stratagene Mx3005P quantitative PCR system thermocycler.

Western blotting and TCA precipitation

Western blotting (38) and TCA precipitation (14) were done as previously described. The Abs used for Western blotting were biotinylated anti–human ULBP2 (R&D Systems, BAF1298), anti-ERK1 (Santa Cruz Biotechnology, sc-93), anti-CD74/Ii (Novus Biologicals, NBP1-33109), anti-GAPDH (Fitzgerald, 10R-G109a), streptavidin-peroxidase polymer (ultrasensitive) (Sigma-Aldrich, 2438), peroxidase-conjugated rabbit anti-mouse Igs (Dako, P0260), and peroxidase-conjugated swine anti-rabbit Igs (Dako, P0399). TCA-precipitated samples were diluted in NuPAGE LDS sample buffer and Western blotting was performed against ULBP2. Serum proteins from culture supernatants were stained with amido black (Sigma-Aldrich, A8181) according to the manufacturer's protocol.

Flow cytometry

Ab cell surface staining (39) and annexin V staining (38) were done as previously described. The following Abs were used: PE-conjugated mouse anti–human (h) MICA/B (BD Biosciences, 558352), PE-conjugated mouse anti–hICAM-1 (Leinco Technologies, C170), PE-conjugated mouse anti-hULBP2/5/6 (R&D Systems, FAB1298P), PE-conjugated mouse anti-hHLADQ1 (BioLegend, 318105), allophycocyanin-conjugated goat anti–mouse IgG (BioLegend, 405308), allophycocyanin-conjugated mouse anti-hULBP2/5/6 (R&D Systems, FAB1298A), allophycocyanin-conjugated anti-hNKG2D (R&D Systems, FAB139A), allophycocyanin-conjugated anti-hCD4, clone OKT4 (BioLegend, 317416), and anti-myc tag, clone 4A6 (Millipore, 05-724). The binding of recombinant hNKG2D-Fc (R&D Systems, 1299-NK) was detected by using a secondary, FITC-conjugated rabbit anti-hIgG (Dako, F0185). Appropriate IgG isotype controls were purchased from BD Biosciences. The flow cytometry data acquisition was performed with an Accuri C6 flow cytometer and CFlow software, and the analyses of the collected data were carried out in FCS Express 3.0. All samples were analyzed by gating on viable cells followed by exclusion of duplets. All results show forward scatter on a linear scale and fluorescence on a $\log_{10}$ scale.

Confocal microscopy

Localization of the ULBP2 construct was investigated by transiently transfecting 1×10^6 Jurkat Tag-9 cells with 3 μg ULBP2-GFP as described above. Two hours after transfection, cells were either treated with 5 μM MSA or kept untreated and incubated for 18 h. For labeling and tracking of acetic organelles, 1 ml transfected Jurkat Tag-9 cells were stained with 1 μl LysoTracker Red DND-99 for 20 min. Images were recorded using a Zeiss CellObserver equipped with a Yokogawa CSU-X1 spinning disk acquiring full Z-stacks of the cells in two channels (EGFP and LysoTracker Red DND-99) using an alpha Plan-Apochromat oil ×100/1.46 numerical aperture objective (Carl Zeiss, Jena, Germany) with an exposure time of 100 ms for each channel. Cells were analyzed at 37°C in culture medium. Single images from the stacks were selected for figures and these were postprocessed using a median filter to minimize noise.

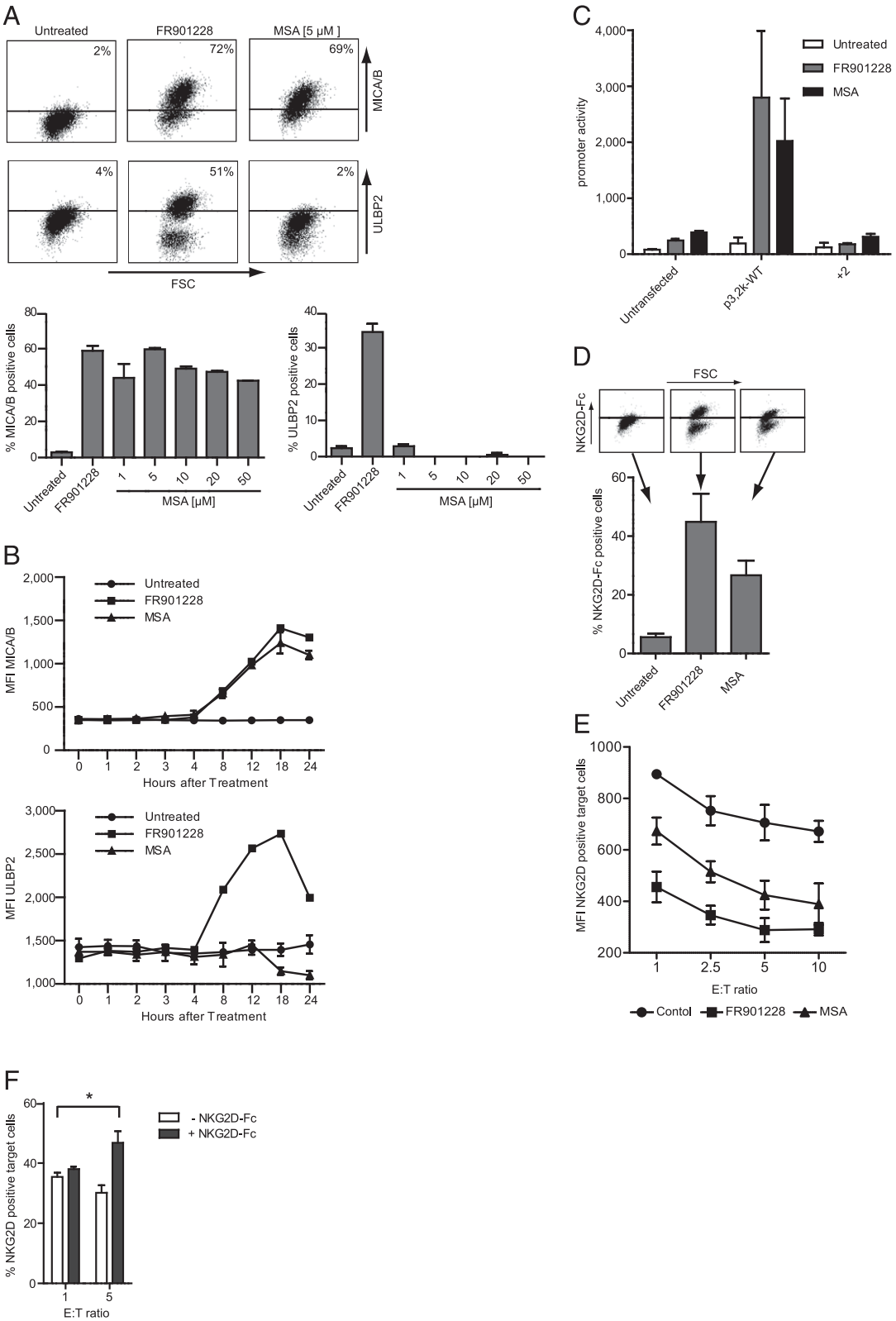

FIGURE 1. MSA induces functional MICA/B expression. (**A**) Jurkat E6-1 cells were left untreated or treated with 20 ng/ml FR901228 or various concentrations of MSA (1, 5, 10, 20, 50 μM). After 18 h, cells were analyzed for MICA/B and ULBP2 cell surface expression by flow cytometry. FR901228 was used as a positive control for MICA/B and ULBP2 induction. (**B**) Jurkat E6-1 cells were treated for the indicated time points with 20 ng/ml FR901228 or 5 μM MSA. At the indicated time points cells were analyzed for MICA/B and ULBP2 cell surface expression by flow cytometry. (**C**) Jurkat Tag-9 cells were transfected with either the 3.2-kb wild-type MICA promoter construct or the +2 control construct. After 24 h cells were treated with 20 ng/ml FR901228 or 5 μM MSA for 18 h. Cells were analyzed for GFP fluorescence by flow cytometry. (**D**) Jurkat E6-1 cells were treated with 20 ng/ml FR901228 or 5 μM MSA. After 18 h cells were analyzed for NKG2D-Fc surface expression by flow cytometry. (**E**) Jurkat E6-1 cells were treated with 20 ng/ml FR901228 or 5 μM MSA. After 12 h cells were cocultured with 3-d-old and IL-15–activated CD8 T cells. After 1 h CD8 T cells were analyzed for NKG2D surface expression by flow cytometry. (**F**) Jurkat E6-1 cells were treated with 5 μM MSA. Twelve hours later interaction of NKG2D ligands and NKG2D receptor was blocked by preincubating the cells for 30 min at 4˚C with hNKG2D-Fc or a vehicle control. Cells were (*Figure legend continues*)

Statistical analysis

Data in Figs. 3A and 6B were analyzed by one-way ANOVAs with a Tukey multiple comparisons test to determine significant differences among groups. Data in Figs. 1F, 4B, 6D, 7A, and 7C were investigated by regular two-way ANOVAs with a Tukey post hoc test for multiple comparisons. Unpaired, two-sided *t* tests were applied to investigate the silencing effect of CD74 siRNAs compared with controls (Fig. 7D). Data are presented as means ± SD and the level of statistical significance was set at $p < 0.05$ for all experiments. The statistical analysis and graph preparation was performed using the software package Prism version 6 (GraphPad Software, La Jolla, CA).

Results

MSA induces functional MICA/B expression

Through database and literature searches as well as compound screenings performed in our laboratory, we uncovered similarities in the gene-activation profiles after MSA and HDAC inhibitor treatment. Therefore, we examined whether MSA, similar to HDAC inhibitors, could induce NKG2D ligands (39). MSA is a stable, synthetic selenium compound, which is known to exhibit anticancer and chemopreventive properties, including the inhibition of tumor growth (40), modification of metastasis (41), and the induction of apoptosis (42). Jurkat T cells have a low MICA/B expression and an intermediate basal level of ULBP2. Treatment of Jurkat E6-1 cells for 18 h with different concentrations of MSA or the HDAC inhibitor FR901228 showed that both treatments caused MICA/B induction, whereas only FR901228 increased ULBP2 surface expression (Fig. 1A). MSA induced MICA/B with a similar expression kinetic as FR901228; surface expression was detected after 4 h and climbed to a maximum at ~12–18 h (Fig. 1B). MSA was not associated with any surface expression of ULBP2 from 0 to 24 h, demonstrating that the lack of ULBP2 expression is not due to an altered kinetic expression profile. These data indicate that expression of MICA/B and ULBP2 are regulated by different mechanisms. MSA further directly stimulated a transiently transfected MICA promoter construct; no promoter activity was observed when using a promoterless variant (+2) (Fig. 1C). It was important to exclude the possibility that MSA-mediated MICA/B expression was caused by stress of dying cells. We therefore stained apoptotic cells with annexin V in combination with Abs against MICA/B, ULBP2, or an isotype control. Only annexin V^- cells upregulated NKG2D ligands after MSA or FR9011228 treatment, suggesting that NKG2D ligand expression is confined to the nonapoptotic cell fraction (data not shown). To examine the integrity of MSA-induced MICA/B proteins, we tested their ability to interact with the native NKG2D receptor. Jurkat E6-1 cells were treated with either MSA or FR901228 and labeled with recombinant hNKG2D-Fc. MSA induced functional NKG2D ligand surface expression that could be detected with recombinant NKG2D-Fc (Fig. 1D). NKG2D also binds to ULBP1–6, which may explain the differences in NKG2D-Fc binding because MSA, in contrast to FR901228, does not induce ULBP2. The NKG2D receptor on CD8 T cells is internalized after interaction with NKG2D ligands (20). To further assess the functional ability of MSA-induced NKG2D ligands, we examined NKG2D downregulation on IL-15–activated CD8 T cells isolated from peripheral blood. An increasing ratio of both FR901228- and MSA-treated Jurkat E6-1 cells triggered a marked reduction in NKG2D surface expression compared with vehicle-treated control cells (Fig. 1E). To verify that downregulation of NKG2D is specifically caused by MSA-induced NKG2D ligands, we preincubated MSA-treated effector Jurkat E6-1 cells with hNKG2D-Fc to block interaction of NKG2D ligands and NKG2D receptor during coculture. As expected, hNKG2D-Fc–treated effector cells caused no downregulation of NKG2D on CD8 T cells compared with vehicle-treated control cells (Fig. 1F). In a similar experiment, Abs against ULBP2 and MICA/B also blocked NKG2D downregulation (data not shown).

This suggests that MSA-mediated MICA/B surface expression is functional and able to specifically downmodulate NKG2D on peripheral blood CD8 T cells.

MSA induces ULBP2 mRNA transcription but abrogates ULBP2 protein expression

Combined treatment with MSA and FR901228 resulted in enhanced surface expression of MICA/B. Surprisingly, FR901228-mediated ULBP2 expression was effectively blocked by MSA cotreatment (Fig. 2A). MSA treatment also inhibited ULBP2 surface expression induced by the HDAC inhibitors SAHA, TSA, and butyrate (Fig. 2B). To clarify how MSA regulates NKG2D ligands, real-time PCR analyses of MICA and ULBP2 mRNA were performed after treatment with MSA, FR901228, or the combination. As expected, the treatment with MSA and FR901228 increased MICA mRNA. Interestingly, MSA treatment caused an accumulation of ULBP2 mRNA similar to FR901228 treatment, and the combination of the two compounds showed no sign of inhibition at the mRNA level (Fig. 2C). Western blotting of whole-cell lysates showed that ULBP2 protein expression was inhibited after treatment with MSA alone or in combination with FR901228 (Fig. 2D). Similar results were observed by intracellular staining for ULBP2 by flow cytometry (data not shown).

These data suggest that MSA and FR901228 induce similar MICA/B and ULBP2 gene regulation. The MSA-mediated ULBP2 mRNA does not result in ULBP2 protein or surface expression and further dominantly suppresses HDAC inhibitor–induced ULBP2.

MSA inhibits ULBP2 protein surface transport

To examine whether MSA inhibits ULBP2 at the posttranslational level, we transiently overexpressed a ULBP2-GFP-myc construct in Jurkat Tag-9 cells. Cells were treated with either FR901228, MSA, or in combination and surface expression of the ULBP2-GFP-myc construct was analyzed by flow cytometry and staining against the myc-tag. Surface expression of the ULBP2 construct was decreased after MSA treatment (Fig. 3A). The ULBP2-GFP level was similar after all treatments (data not shown), suggesting that ULBP2 is retained intracellularly but not degraded during the timeframe of the assay. This was confirmed by an anti-GFP Western blot of the transfected cells where no GFP degradation was observed (Fig. 3B). To further examine the intracellular retention of ULBP2, we used live cell confocal microscopy. This experiment revealed that transfected ULBP2 accumulated around the nucleus of Jurkat Tag-9 cells and was not expressed on the cell surface (Fig. 3C, *right*) compared with untreated cells (Fig. 3C, *left*).We also investigated the effect of FR901228 and MSA on Jurkat Tag-9 cells transiently transfected with a GFP-MICA*018 plasmid by flow cytometry and confocal microscopy. FR901228 and MSA both induced surface expression of GFP-MICA*018 compared with untreated cells (data not shown). These data

then cocultured with 3-d-old and IL-15–activated CD8 T cells. After 2 h CD8 T cells were analyzed for NKG2D surface expression by flow cytometry. Data are representative of at least three separate experiments [(A)–(D); (E) and (F) from three donors, means ± SD]. $*p < 0.05$.

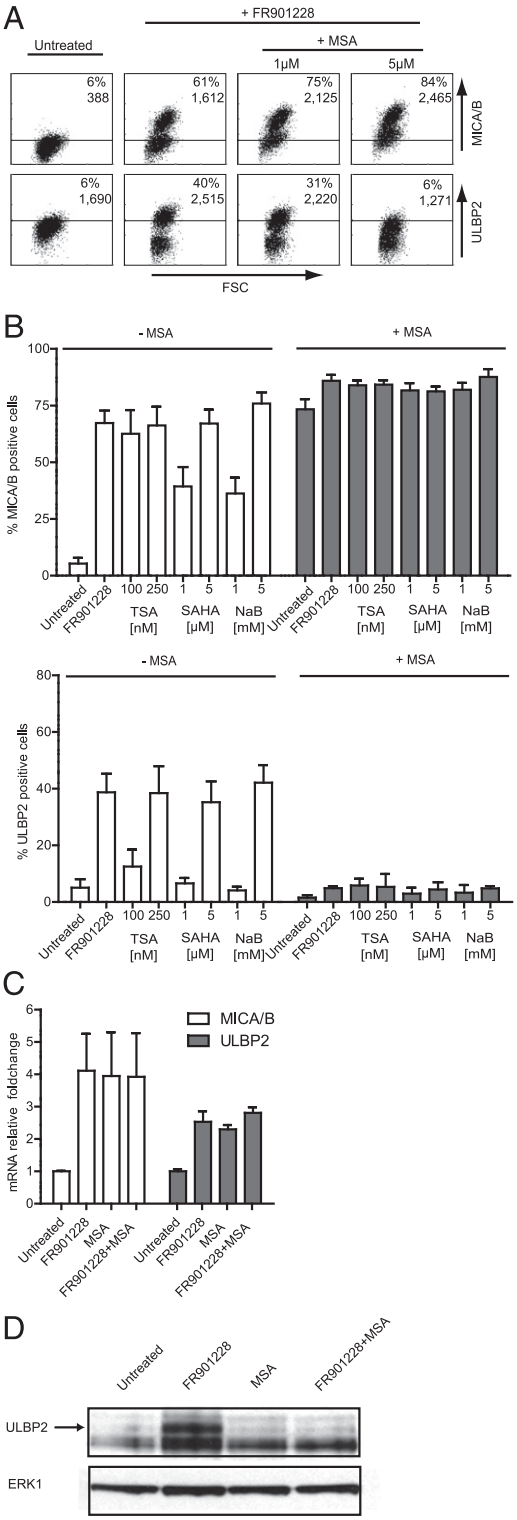

FIGURE 2. MSA induces ULBP2 mRNA transcription but abrogates ULBP2 protein expression. (**A**) Jurkat E6-1 cells were left untreated or treated with either 20 ng/ml FR901228 or 5 μM MSA alone or in combination with 20 ng/ml FR901228. After 18 h cells were analyzed for MICA/B and ULBP2 surface expression by flow cytometry. Cells were gated according to untreated cells. (**B**) Jurkat E6-1 cells were treated with various concentrations of three different HDAC inhibitors (TSA, SAHA, and sodium butyrate [NaB]) alone or in combination with 5 μM MSA. Treatment with FR901228 was used as a positive control for MICA/B and ULBP2 induction. After 18 h cells were analyzed for MICA/B (*top*) and ULBP2 (*bottom*) surface expression by flow cytometry. (**C**) Jurkat E6-1 cells were left untreated or treated with 20 ng/ml FR901228, 5 μM MSA, or a combination of both. After 4 h total RNA was extracted and used for quantitative real-time PCR analysis. MICA and ULBP2 mRNA expression was normalized to the housekeeping gene (*RPLP0*) and displayed as the fold change relative to the control. (**D**) Jurkat E6-1 cells were left untreated or treated with 20 ng/ml FR901228, 5 μM MSA, or a combination. After 18 h cells were lysed and used for Western blotting against ULBP2 (*top*; molecular mass of 35 kDa) and ERK1 (*bottom*; molecular mass of 44 kDa). Data are representative of four separate experiments [(A)–(C), means ± SD] or three experiments (D).

strongly suggest that MSA inhibits ULBP2 surface expression through a posttranslational mechanism.

MSA regulates NKG2D ligand expression in different cancers and activated CD4 T cells

Different cell lines were examined for their response to MSA. As expected (39), HDAC inhibitor treatment increased the surface expression of MICA/B and ULBP2 in HEK293T, PC3 prostate cancer, and U373 glioma cells (Fig. 4A), although U373 cells had low induction of MICA/B surface expression. MSA treatment alone or in combination with FR901228 gave the same phenotype as described above for Jurkat E6-1 cells, that is, an increase in MICA/B but dominant inhibition of ULBP2 surface expression (Fig. 4A). We have previously shown that healthy activated CD4 T cells obtained from peripheral blood cells express MICA/B after HDAC inhibitor treatment (39). In the present study, we further show that ULBP2 is also induced on CD4 T cells after FR901228 treatment. MSA strongly induced MICA/B surface expression; however, it caused only a low induction of ULBP2 surface expression (Fig. 4B).

MSA is able to inhibit the production of soluble ULBP2 from primary melanoma cells

Prostate cancer, B-CLL leukemia, and melanomas evade immune recognition by releasing soluble ULBP2 into the extracellular environment, rendering the tumor cells undetectable by NKG2D-expressing immune effector cells (19, 22, 23). Therefore it was of interest, also for a future therapeutic potential, to examine whether MSA hinders the production of soluble ULBP2 and thereby overcomes a well-known tumor escape mechanism. Three different primary melanoma cell lines were examined. MSA inhibited ULBP2 surface expression as expected (Fig. 5A). To test the effect of MSA on soluble ULBP2, we precipitated proteins from melanoma cell culture supernatants using TCA after an 18-h treatment with/or without FR901228, MSA, or the combination. All primary melanomas constitutively produced soluble ULBP2, and the level of soluble ULBP2 was further enhanced by FR901228 treatment. Interestingly, MSA treatment inhibited both the constitutive and induced soluble ULBP2 expression below the detection limit of Western blot analysis. In contrast to our previous findings, MSA alone or in combination with FR901228 also inhibited the surface expression of MICA/B in melanomas. This interesting finding is further studied in the following sections.

ULBP2 induction is dependent on PKC activation

Previous studies have shown that MSA specifically inactivates PKC isoenzymes (43). To determine whether ULBP2 expression involves PKC activation, we treated Jurkat E6-1 cells with the two PKC activators PMA and ingenol. Interestingly, both PMA and ingenol treatment for 18 h caused a robust ULBP2 surface expression without affecting MICA/B surface expression (Fig. 6A). We also exposed Jurkat E6-1 cells to the ingenol derivative ingenol-3-angelate, a more potent PKC activator than ingenol but

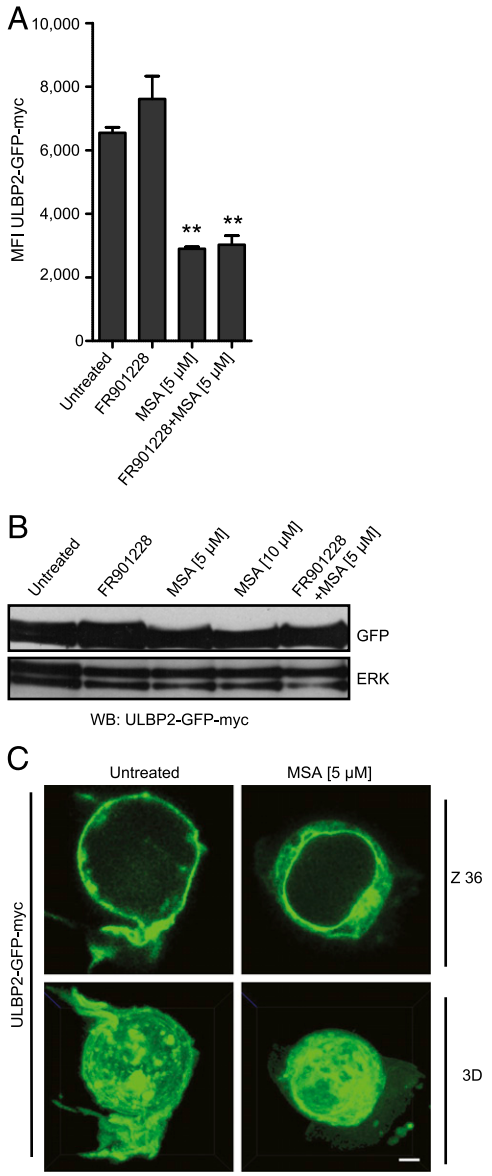

FIGURE 3. MSA inhibits ULBP2 protein surface transport. (**A**) Jurkat Tag-9 cells were transiently transfected with the ULBP2-myc-GFP construct. Two hours posttransfection cells were left untreated or treated with either 20 ng/ml FR901228, 5 μM MSA, or a combination of both. After 18 h cells were analyzed for myc-tag cell surface expression by flow cytometry. Cells were gated according to nontransfected cells. (**B**) Jurkat Tag-9 cells were transiently transfected with the ULBP2-myc-GFP construct. Two hours posttransfection cells were left untreated or treated with various concentrations of MSA (5 or 10 μM). After 18 h cells were lysed and used for Western blotting against GFP (*top*, molecular mass of ~64 kDa) and ERK1 (*bottom*, molecular mass of 44 kDa). (**C**) Jurkat Tag-9 cells were transiently transfected with the ULBP2-myc-GFP construct. Two hours posttransfection cells were left untreated or treated with 5 μM MSA. After 18 h, cell images were recorded using a Zeiss CellObserver equipped with a Yokogawa CSU-X1 spinning disk acquiring full Z-stacks of the cells in the EGFP channel using an alpha Plan-Apochromat oil ×100/1.46 numerical aperture objective. Z-stacks at position 36 were chosen to compare construct location in untreated cells (*left top*) and MSA-treated cells (*right top*). Full Z-stacks were used to create three-dimensional images of the construct location in untreated cells (*left bottom*) and MSA-treated cells (*right bottom*). Scale bar, 2 μm. Data are representative of four separate experiments [(A), means ± SD] or two experiments (B and C). $^{**}p < 0.01$.

with a shorter half-life (44). A single exposure of ingenol-3-angelate for 18 h did not induce ULBP2 surface expression. In contrast, two or four sequential additions upregulated ULBP2 surface expression, although not as potently as the more sustained PKC activators PMA and ingenol (Fig. 6B). Kinetic studies showed that ULBP2 surface expression was highest after 18 h of treatment with PMA (Fig. 6C), which is consistent with our previous findings with FR901228 (39). Again, MICA/B surface expression was not affected throughout the PMA stimulation (Fig. 6C). To verify the involvement of PKC activity, we examined

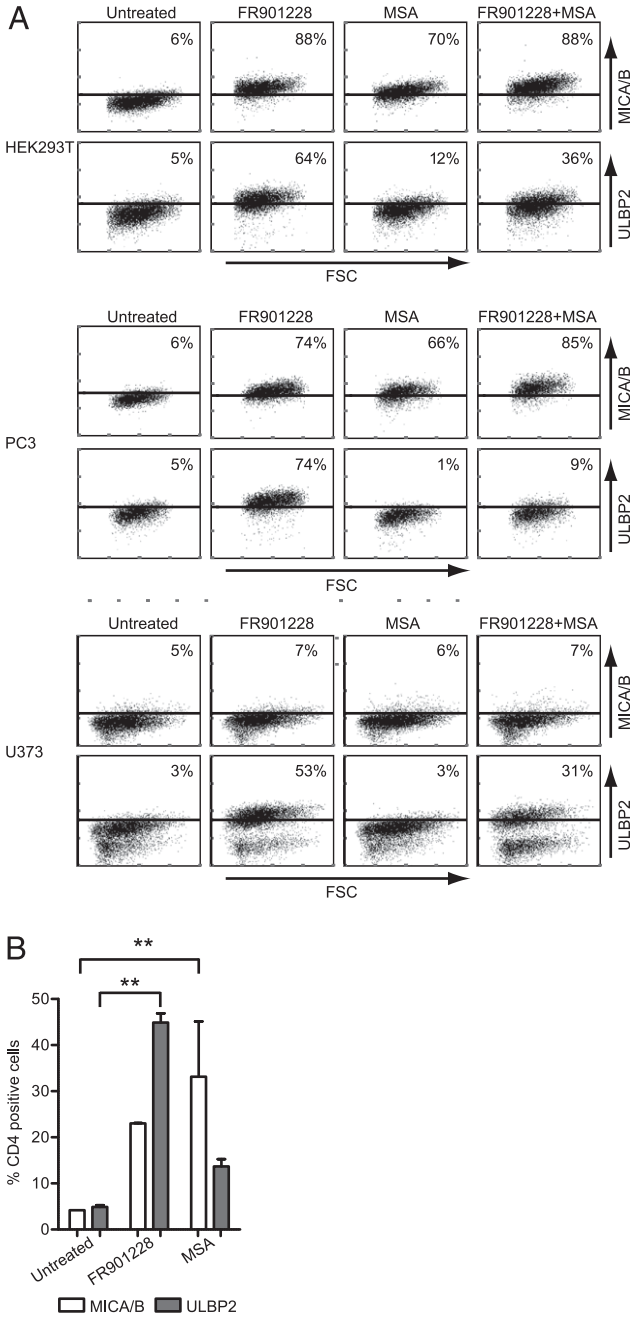

FIGURE 4. MSA regulates NKG2D ligand expression in different cancers and activated CD4 T cells. (**A**) HEK293T, PC3, and U373 cells were left untreated or either treated with 20 ng/ml FR901228 or with 25, 10, and 5 μM MSA, respectively, alone or in combination. After 18 h cells were analyzed for MICA/B and ULBP2 surface expression by flow cytometry. (**B**) Restimulated $CD4^+$ T cells as described in *Materials and Methods* were left untreated or either treated with 20 ng/ml FR901228 or with 10 (white) and 5 (gray) μM MSA. After 18 h cells were analyzed for MICA/B and ULBP2 surface expression by flow cytometry. Data are representative of at least three separate experiments [(A), means ± SD)] or three experiments (three donors) [(B), means ± SD]. $^{**}p < 0.01$.

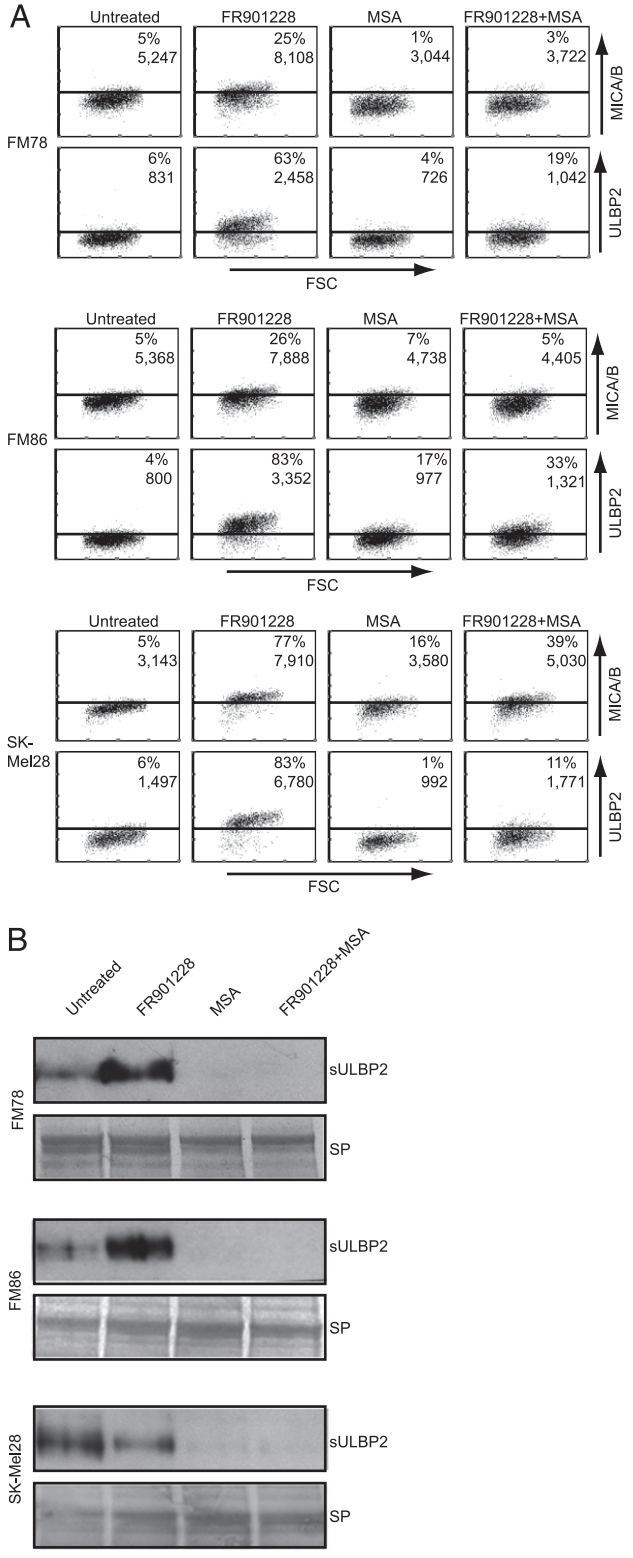

FIGURE 5. MSA is able to inhibit the production of soluble ULBP2 in primary melanoma cells. (**A**) FM-78, FM-86, and SK-MEL28 were left untreated or either treated with 20 ng/ml FR901228 or 10 μM MSA alone or in combination. After 18 h cells were analyzed for MICA/B and ULBP2 surface expression by flow cytometry. (**B**) FM-78 (*top*), FM-86 (*middle*), and SK-MEL28 (*bottom*) cells were left untreated or treated with either 20 ng/ml FR901228 or 10 μM MSA alone or in combination for 18 h using culture medium containing 0.5% FBS. The proteins in the media fraction were precipitated by TCA as described in *Materials and Methods*. Western blotting of precipitates was performed using an Ab against ULBP2 (*top*; molecular mass of 35 kDa). Serum proteins (SP) (*bottom*; molecular mass of 170 kDa) from culture supernatants were stained with amido black and used as loading controls. Data are representative of three separate experiments (A and B).

whether inhibitors of PKC affected ULBP2 surface expression. We used the potent PKC inhibitor Gö 6976 (Fig. 6D, *right*) and the broad-spectrum PKC inhibitor Gö 6983 (Fig. 6D, *left*). Because both PKC inhibitors are short-lived they were added initially together with FR901228 or PMA and then again 4–6 h later. Both inhibitors efficiently blocked ULBP2 surface expression after PMA treatment (Fig. 6D). The PKC inhibitors also inhibited FR901228 surface-induced ULBP2, but not as efficiently as after PMA exposure. The PKC inhibitors had no effect on FR901228-induced MICA/B expression (data not shown). These data suggest that PKC activity is indeed involved in ULBP2 expression; however, the data also indicate that HDAC inhibitors and PKC activators may not regulate ULBP2 surface expression through identical PKC isoforms. As expected, MSA potently blocked PMA-induced ULBP2 surface expression (Fig. 6E), confirming the PKC inhibitory potential of MSA.

The lysosomal/endosomal transport pathway is important for ULBP2 cell surface expression

PKC activity is known to be crucial for lysosomal/endosomal intracellular transport (45, 46), prompting us to investigate the involvement of this pathway in ULBP2 regulation. It was therefore interesting to examine whether ULBP2 surface transport could be selectively dependent on this pathway. FR901228-induced ULBP2 surface expression, but not MICA/B, was efficiently blocked by three different inhibitors of lysosomal acidification (Fig. 7A). PMA-induced ULBP2 was also blocked by inhibition of lysosomal acidification (data not shown). Using live cell confocal microscopy, we examined whether ULBP2 was retained in lysosomal/endosomal compartments after chloroquine treatment (Fig. 7B). Jurkat Tag-9 cells were transiently transfected with constructs encoding GFP-myc–tagged ULBP2 or MICA*018, and LysoTracker Red was used to stain for lysosomal/endosomal compartments. Indeed, the transiently expressed ULBP2 was completely retained in the lysosomes (Fig. 7B, *top*), whereas MICA*018 was localized on the cell surface (Fig. 7B, *bottom*). A significant part of the MICA*018 protein also colocalized with the LysoTracker; whether this is due to lysosomal MICA*018 degradation or low resolution between the ER/Golgi and lysosomal compartments is not clear from our results.

MSA also inhibited MICA/B surface expression in primary melanoma cells, suggesting that MICA/B in this circumstance may use the same pathway as ULBP2 for surface expression. Indeed, bafilomycin A inhibited both ULBP2 and MICA/B surface expression in the primary FM-86 melanoma cells (Fig. 7C). Similar results were obtained with chloroquine and ammonium chloride (data not shown). These results emphasize that MICA/B, under special circumstances, may use the lysosomal/endosomal pathway for surface transport. This might be the case when the conventional transport pathway is blocked, as has been demonstrated for some melanomas (15).

The invariant chain facilitates endosomal transport and surface expression of ULBP2

Ii can transport certain MHC class I homologous molecules to the cell surface through an endosomal pathway, with MR1 and CD1d being prominent examples (32, 34). Because NKG2D ligands are MHC class I homologs, we tested the influence of Ii for ULBP2

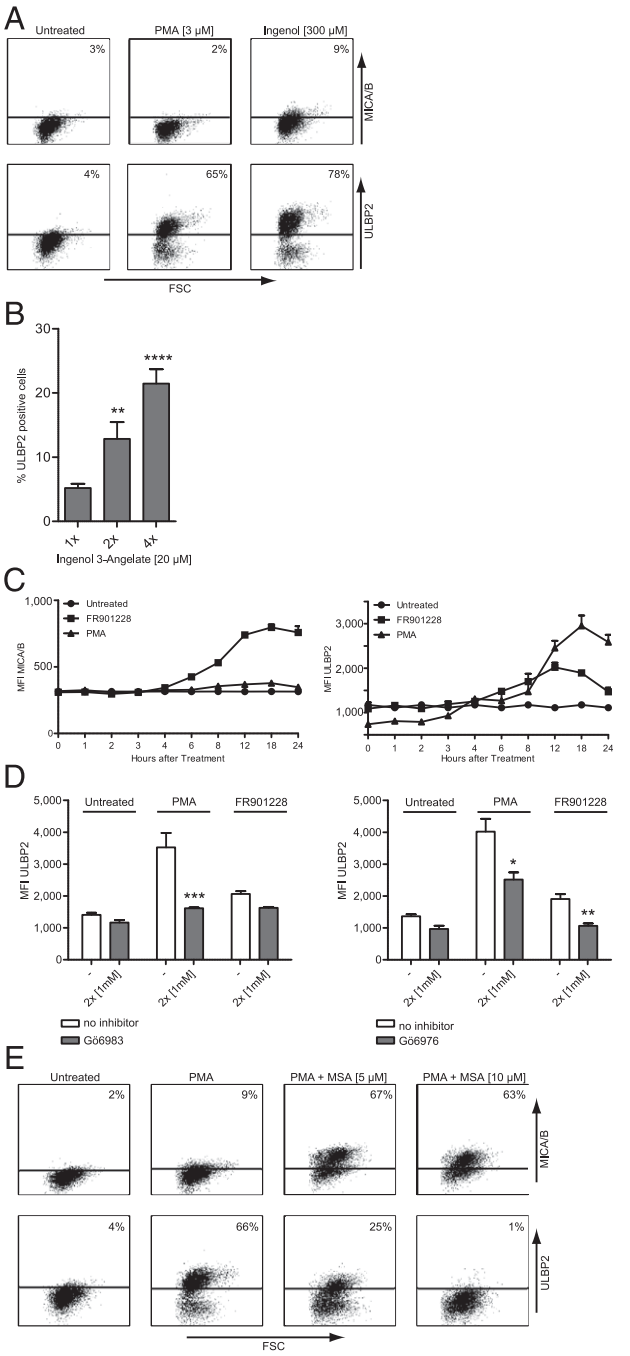

FIGURE 6. ULBP2 induction is dependent on PKC activation. (**A**) Jurkat E6-1 cells were left untreated or incubated with 3 μM PMA or 300 μM ingenol. After 18 h cells were analyzed for MICA/B and ULBP2 surface expression by flow cytometry. (**B**) Jurkat E6-1 cells were left untreated or treated once, twice, or four times with 20 μM ingenol-3-angelate during a time period of 16 h. After incubation cells were analyzed for ULBP2 surface expression by flow cytometry. (**C**) Jurkat E6-1 cells were treated for the indicated time points with 20 ng/ml FR901228 or 3 μM PMA. At the indicated time points cells were analyzed for MICA/B and ULBP2 cell surface expression by flow cytometry. (**D**) Jurkat E6-1 cells were left untreated or treated with 3 μM PMA or 20 ng/ml FR901228 alone or in combination with 1 mM of the PKC inhibitors Gö6983 (*left*) or Gö6976 (*right*). The PKC inhibitors were added to the cell culture for the first time together with FR901228 or PMA and for the second time 4–6 h later. After 18 h, cells were analyzed for ULBP2 surface expression by flow cytometry. (**E**) Jurkat E6-1 cells were left untreated or treated with 3 μM PMA alone or in combination with either 5 or 10 μM MSA. After 18 h, cells were analyzed for MICA/B and ULBP2 surface expression by flow cytometry. Data are representative of at least three separate experiments [(A) and (C)–(E), means ± SD] or two separate experiments [(B), means ± SD]. $*p < 0.05$, $**p < 0.01$, $***p < 0.001$, $****p < 0.0001$.

and MICA/B surface expression. Ii expression in Jurkat Tag-9 cells was knocked down using two different siRNAs targeting all isoforms of Ii. In both cases, Ii knockdown significantly inhibited the surface transport of ULBP2 (Fig. 7D, *left*, *top* and *bottom*). Interestingly, MICA/B surface expression was also reduced after Ii silencing, although not to the level observed for ULBP2 (Fig. 7D, *middle*, *top* and *bottom*). Expression of ICAM-1 was not affected and served as a control (Fig. 7D, *right*, *top* and *bottom*). The level of MICA and ULBP2 mRNA was not affected by Ii knockdown (data not shown). Protein knockdown of Ii in Jurkat Tag-9 cells was confirmed by Western blotting (Fig. 7D). To further substantiate the involvement of Ii, we overexpressed an Ii construct in Jurkat Tag-9 cells as well as FM-86 melanoma cells. After transfection, the cells were either treated with FR901228 or kept untreated and the expression of NKG2D ligands was analyzed by flow cytometry (Fig. 7E). In Jurkat Tag-9 cells, the level of both endogenous and FR901228-induced cell-surface ULBP2 was increased by overexpression of Ii (Fig. 7E, *left*, *bottom*). As expected, the surface expression of MICA/B was unaffected (Fig. 7E, *left*, *top*). Strikingly, overexpression of Ii in FM-86 melanoma cells induced both ULBP2 and MICA/B surface expression, with and without FR901228 treatment (Fig. 7E, *right*, *top* and *bottom*). These results thus corroborate that MICA/B expression in melanoma cells can be regulated by Ii. The overexpression of the Ii construct was verified by Western blotting (data not shown). Cotransfection of constructs encoding ULBP2 and Ii enhanced construct-encoded ULBP2 surface expression in both Jurkat Tag-9 and FM-86 cells (data not shown).

It is well established that MHC class II molecules use Ii for cell-surface transport. Thus, we considered whether MSA could be an inhibitor of MHC class II surface expression. To test this, we induced MHC class II surface expression on freshly isolated monocytes with IFN-γ. Endogenous and IFN-γ-induced MHC class II surface expression was potently inhibited by MSA (Fig. 7F), showing that MSA has a potent and unrecognized inhibitory effect on MHC class II surface expression and endosomal transport.

In summary, our data suggest that soluble and surface-expressed ULBP2 is dependent on the endosomal transport pathway. In contrast, MICA/B is trafficked to the cell surface via the conventional ER/Golgi pathway. Interesting exceptions are the investigated melanomas, where MICA/B surface transport is also dependent on the endosomal pathway. This implies that Ii could associate early in the ER with both ULBP2 and MICA/B in a chaperone-like fashion and facilitate surface transport depending on the integrity of the ER/Golgi system.

Discussion

In this study, we show that the NKG2D ligand ULBP2 is transported to the cell surface through an endosomal pathway dependent on PKC and lysosomal integrity. We further reveal that ULBP2 surface transport is dependent on the invariant chain and thus shares the surface transport pathway with MHC class II proteins and several other MHC class I homologous proteins (32, 34).

The endosomal transport pathway of ULBP2 was uncovered by studying the selenium-containing compound MSA. Initially, we noticed a significant overlap in gene expression profiles of cells treated with either HDAC inhibitors or MSA. Hence we examined

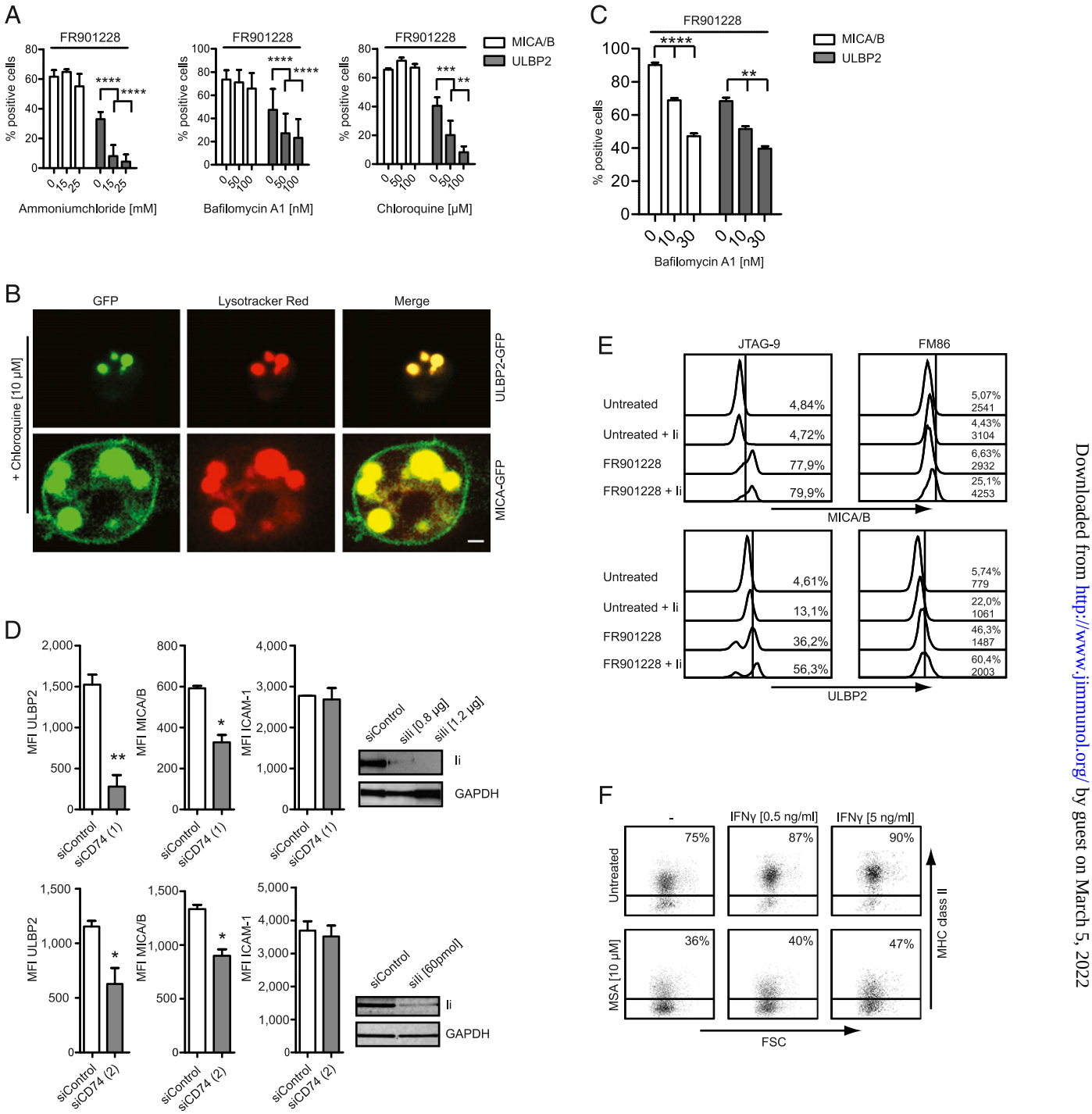

FIGURE 7. The lysosomal/endosomal transport pathway is important for ULBP2 cell surface expression and is facilitated by invariant chain. (**A**) FR901228-treated Jurkat E6-1 cells with lysosomal inhibitors (from *left* to *right*: ammonium chloride, bafilomycin A1, chloroquine) at indicated concentrations. Cells were analyzed for MICA/B and ULBP2 surface expression. (**B**) Jurkat Tag-9 cells were transiently transfected with either the ULBP2-myc-GFP (*top*) or MICA*018-myc-GFP (*bottom*) construct and treated with 10 μM chloroquine for 18 h. For labeling and tracking of the acetic organelles, cells were stained as described in *Materials and Methods*. Images were taken in two channels: enhanced GFP (EGFP; green) and LysoTracker Red DND-99 (red). Colocalization is shown in yellow. Scale bar, 2 μm. (**C**) FR901228-treated FM-86 cells with 10 and 30 nM bafilomycin A1. Cells were analyzed for MICA/B and ULBP2 surface expression. (**D**) Jurkat Tag-9 cells were transfected with two different siRNAs against CD74 or their corresponding siRNA control. Six hours posttransfection cells were treated with 20 ng/ml FR901228. After 18 h half of the cells were analyzed for ULBP2 (*left*), MICA/B (*middle*), and ICAM-I (*right*) surface expression. The remaining cells were lysed and used for Western blotting against Ii (molecular mass of ~43 kDa) and GAPDH (molecular mass of 37 kDa). (**E**) Jurkat Tag-9 cells and FM-86 cells were transfected with an Ii construct or a control plasmid. After 24 h cells were treated with FR901228 or kept untreated for 18 h. Cells were analyzed for MICA/B and ULBP2 surface expression. (**F**) IFN-γ–stimulated (0.5 or 5 ng/ml) and nonstimulated monocytes were left untreated or treated with 10 μM MSA (18 h). Cells were analyzed for MHC class II surface expression. Data are representative of at least three separate experiments [(A) and (C)–(F), means ± SD] or two separate experiments (B). $*p < 0.05$, $**p < 0.01$, $***p < 0.001$, $****p < 0.001$.

whether MSA, similar to HDAC inhibitors, caused gene activation and surface expression of NKG2D ligands (39). Our results show a remarkable action of MSA, including 1) gene activation and upregulation of MICA/B surface expression and 2) ULBP2 gene activation, however, combined with a dominant suppression of ULBP2 protein secretion and surface expression. Our mechanistic studies further suggest that MSA inhibits endosomal ULBP2 transport through sustained inhibition of PKC activity.

MSA induction of ULBP2 mRNA strongly suggested that inhibition of ULBP2 expression occurs posttranscriptionally. This was confirmed by transient overexpression of ULBP2, where MSA inhibited surface expression of ULBP2. Our studies revealed that PKC activity was essential for ULBP2 surface expression, as different PKC activators and inhibitors regulated ULBP2 surface expression. It is noticeable that prolonged PKC activity was important for induction of ULBP2 surface expression because the PKC activator ingenol-3-angelate and the PKC inhibitors Gö 6976 and Gö 6983, which all have relatively short half-lifes, needed sequential addition during the assay period to function (47, 48). This was not the case for the PKC activators PMA and ingenol, which are known for their prolonged stability (49). Therefore, it seems likely that the pronounced ULBP2 inhibitory effect of MSA is due to sustained inhibition of PKC. We propose that the prolonged PKC activation needed for ULBP2 induction ensures that short-term PKC activation, which is involved in many intracellular signals, will not cause aberrant ULBP2 expression. There are at least 10 different isoforms of PKC and the different PKC isoforms often work redundantly (50). Therefore, it is not straightforward to elucidate their precise involvement. We have recently shown that ULBP2 surface expression is particularly dependent on intracellular calcium (38). This implies that calcium-dependent PKC isoforms could be involved in the regulation of ULBP2 surface expression, although this requires further experimental verification. Intracellular lysosomal/endosomal transport is dependent on PKC activity (26, 30, 46). Moreover, it has been shown that PKC activity positively regulates the generation of stable MHC class II complexes (46). Our present studies revealed that PKC activation likely governed a lysosomal/endosomal transport of ULBP2. Different inhibitors of lysosomal acidification potently inhibited ULBP2 surface expression without affecting MICA/B surface expression. ULBP2, therefore, shares surface transport with other MHC class I homologous proteins such as MR1 and CD1 molecules, which also use a lysosomal/endosomal surface transport pathway. MHC class I homologs that use this MHC class II–like pathway often associate and depend on Ii for endosomal localization and transport (32, 34). This was also the case for ULBP2, as siRNA-mediated knockdown of Ii almost completely abrogated ULBP2 surface expression. Strikingly, knockdown of Ii also inhibited ~50% of MICA/B surface expression. This was observed repeatedly by using different siRNAs, and expression of several control proteins was not affected. Furthermore, the overexpression of an Ii construct resulted in a further induction of ULBP2. Therefore, it seems possible that Ii interacts with both MICA/B and ULBP2 early in the ER compartment. Ii facilitates the endosomal export of ULBP2 while possibly acquiring a more chaperone-like function for MICA/B. Further investigations are needed to understand how ULBP2 interacts with Ii. This is particularly interesting because ULBP2, in contrast to MHC class II molecules, will likely not interact with the CLIP portion of Ii. The association between Ii and NKG2D ligands may be further relevant because overexpression of Ii is linked to inflammatory diseases and several forms of cancer. Especially high levels of Ii p35 (one of four isoforms in humans) were found in hairy cell leukemia and some B-CLL patients (51), suggesting that Ii may be an interesting target in cancer immune therapy. Hence, detailed studies about which Ii isoforms regulate NKG2D ligands might be clinically relevant.

It is noteworthy that MSA inhibited both ULBP2 and MICA/B surface expression in the different melanoma cell lines. MSA blocking of MICA/B surface expression was not observed in the other cancer and primary cells examined. This implies that the normal MICA/B transport pathway could be hampered in the investigated melanomas. In agreement with this, melanoma cells have been shown to restrict MICA surface expression despite possessing significant intracellular levels (15). Consequently, MICA/B could associate with Ii and be transported to the surface via the endosomal pathway. This hypothesis is supported by our findings that MICA/B surface expression in the melanomas was blocked by inhibition of lysosomal acidification, a phenotype that was not observed in other cell types investigated. Additionally, overexpression of an Ii construct induced cell surface expression of MICA/B in FM-86 melanoma cells but not in Jurkat Tag-9 cells. Our studies further revealed that MSA inhibited the production of soluble ULBP2 from different primary melanoma cells. Production of soluble NKG2D ligands is used by several cancers to avoid immune recognition (6, 19, 24). The presence of soluble ULBP2 in patient serum samples is a marker for poor prognosis in various types of cancers (19, 22, 23). Our current results show that soluble ULBP2 from melanomas can be inhibited by MSA. Thus, MSA or other compounds that target the endosomal pathway could be used to increase immune recognition of soluble ULBP2-producing cancers. Alternatively, MSA also inhibits MHC class II surface expression and possibly NK/CD8 T cell degranulation. Thus, in vivo administration of MSA requires a potential therapeutic window where MSA effectively blocks ULBP2 secretion without severely compromising immune function. In this regard, it is interesting that previous studies have found in vivo tolerated levels of MSA at 10 μg/kg body weight (52). It is known that functional ULBP2 can also be expressed without GPI anchor on the cell surface (53). In this study ULBP2, however, is GPI-linked because no surface expression was detectable after phosphatidylinositol phospholipase C treatment (data not shown).

The endosomal/lysosomal transport pathway is normally used to transport significant amounts of proteins for exocytosis, degranulation, and secretion. It is also used for PKC-dependent virus budding/virion secretion (54). It is therefore important to consider that the special ULBP2 transport pathway may also be beneficial, for example, to highlight virus budding, which might be particularly advantageous for the immune system when viruses shut down other cellular transport pathways. The down side is that some tumor cells exploit this transport pathway to secrete an extensive amount of immunosuppressive ULBP2.

Acknowledgments

We thank Dr. C. Geisler (Department of International Health, Immunology and Microbiology, University of Copenhagen, Copenhagen, Denmark) for providing the Jurkat Tag-9 cell line, Dr. P. thor Straten (Center for Cancer Immune Therapy, Herlev University Hospital, Herlev, Denmark) for providing the melanoma cell lines, and Dr. A. Hudson (Medical College of Wisconsin, Milwaukee, WI) for providing the U373 cell line. We thank Dr. K. Helin (University of Copenhagen) for the pCMV-Myc plasmid, Dr. M. Wills (University of Cambridge) for the GFP-MICA*018 plasmid, Dr. H. Reyburn (Centro Nacional de Biotecnologia, Madrid) for the ULBP2-Flag plasmid, Dr. N. Koch (University of Bonn, Bonn, Germany) for the invariant chain plasmid, and the Core Facility for Integrated Microscopy (Faculty of Health and Medical Sciences, University of Copenhagen).

Disclosures

The authors have no financial conflicts of interest.

References

1. Bauer, S., V. Groh, J. Wu, A. Steinle, J. H. Phillips, L. L. Lanier, and T. Spies. 1999. Activation of NK cells and T cells by NKG2D, a receptor for stress-inducible MICA. *Science* 285: 727–729.
2. Groh, V., A. Bruhl, H. El-Gabalawy, J. L. Nelson, and T. Spies. 2003. Stimulation of T cell autoreactivity by anomalous expression of NKG2D and its MIC ligands in rheumatoid arthritis. *Proc. Natl. Acad. Sci. USA* 100: 9452–9457.
3. Groh, V., K. Smythe, Z. Dai, and T. Spies. 2006. Fas-ligand-mediated paracrine T cell regulation by the receptor NKG2D in tumor immunity. *Nat. Immunol.* 7: 755–762.
4. Vivier, E., E. Tomasello, and P. Paul. 2002. Lymphocyte activation via NKG2D: towards a new paradigm in immune recognition? *Curr. Opin. Immunol.* 14: 306–311.
5. Champsaur, M., and L. L. Lanier. 2010. Effect of NKG2D ligand expression on host immune responses. *Immunol. Rev.* 235: 267–285.
6. Groh, V., R. Rhinehart, J. Randolph-Habecker, M. S. Topp, S. R. Riddell, and T. Spies. 2001. Costimulation of CD8αβ T cells by NKG2D via engagement by MIC induced on virus-infected cells. *Nat. Immunol.* 2: 255–260.
7. Groh, V., J. Wu, C. Yee, and T. Spies. 2002. Tumour-derived soluble MIC ligands impair expression of NKG2D and T-cell activation. *Nature* 419: 734–738.
8. Raffaghello, L., I. Prigione, I. Airoldi, M. Camoriano, I. Levreri, C. Gambini, D. Pende, A. Steinle, S. Ferrone, and V. Pistoia. 2004. Downregulation and/or release of NKG2D ligands as immune evasion strategy of human neuroblastoma. *Neoplasia* 6: 558–568.
9. Routes, J. M., S. Ryan, K. Morris, R. Takaki, A. Cerwenka, and L. L. Lanier. 2005. Adenovirus serotype 5 E1A sensitizes tumor cells to NKG2D-dependent NK cell lysis and tumor rejection. *J. Exp. Med.* 202: 1477–1482.
10. Andresen, L., H. Jensen, M. T. Pedersen, K. A. Hansen, and S. Skov. 2007. Molecular regulation of MHC class I chain-related protein A expression after HDAC-inhibitor treatment of Jurkat T cells. *J. Immunol.* 179: 8235–8242.
11. Bauman, Y., D. Nachmani, A. Vitenshtein, P. Tsukerman, N. Drayman, N. Stern-Ginossar, D. Lankry, R. Gruda, and O. Mandelboim. 2011. An identical miRNA of the human JC and BK polyoma viruses targets the stress-induced ligand ULBP3 to escape immune elimination. *Cell Host Microbe* 9: 93–102.
12. Nachmani, D., D. Lankry, D. G. Wolf, and O. Mandelboim. 2010. The human cytomegalovirus microRNA miR-UL112 acts synergistically with a cellular microRNA to escape immune elimination. *Nat. Immunol.* 11: 806–813.
13. Textor, S., N. Fiegler, A. Arnold, A. Porgador, T. G. Hofmann, and A. Cerwenka. 2011. Human NK cells are alerted to induction of p53 in cancer cells by upregulation of the NKG2D ligands ULBP1 and ULBP2. *Cancer Res.* 71: 5998–6009.
14. Andresen, L., S. L. Skovbakke, G. Persson, M. Hagemann-Jensen, K. A. Hansen, H. Jensen, and S. Skov. 2012. 2-deoxy D-glucose prevents cell surface expression of NKG2D ligands through inhibition of *N*-linked glycosylation. *J. Immunol.* 188: 1847–1855.
15. Fuertes, M. B., M. V. Girart, L. L. Molinero, C. I. Domaica, L. E. Rossi, M. M. Barrio, J. Mordoh, G. A. Rabinovich, and N. W. Zwirner. 2008. Intracellular retention of the NKG2D ligand MHC class I chain-related gene A in human melanomas confers immune privilege and prevents NK cell-mediated cytotoxicity. *J. Immunol.* 180: 4606–4614.
16. Nice, T. J., W. Deng, L. Coscoy, and D. H. Raulet. 2010. Stress-regulated targeting of the NKG2D ligand Mult1 by a membrane-associated RING-CH family E3 ligase. *J. Immunol.* 185: 5369–5376.
17. Renszel, K. M., R. S. Traister, and W. P. Lynch. 2013. Unique *N*-linked glycosylation of CasBrE Env influences its stability, processing, and viral infectivity but not its neurotoxicity. *J. Virol.* 87: 8372–8387.
18. Welte, S. A., C. Sinzger, S. Z. Lutz, H. Singh-Jasuja, K. L. Sampaio, U. Eknigk, H. G. Rammensee, and A. Steinle. 2003. Selective intracellular retention of virally induced NKG2D ligands by the human cytomegalovirus UL16 glycoprotein. *Eur. J. Immunol.* 33: 194–203.
19. Paschen, A., A. Sucker, B. Hill, I. Moll, M. Zapatka, X. D. Nguyen, G. C. Sim, I. Gutmann, J. Hassel, J. C. Becker, et al. 2009. Differential clinical significance of individual NKG2D ligands in melanoma: soluble ULBP2 as an indicator of poor prognosis superior to S100B. *Clin. Cancer Res.* 15: 5208–5215.
20. Song, H., J. Kim, D. Cosman, and I. Choi. 2006. Soluble ULBP suppresses natural killer cell activity via down-regulating NKG2D expression. *Cell. Immunol.* 239: 22–30.
21. Ashiru, O., P. Boutet, L. Fernández-Messina, S. Agüera-González, J. N. Skepper, M. Valés-Gómez, and H. T. Reyburn. 2010. Natural killer cell cytotoxicity is suppressed by exposure to the human NKG2D ligand MICA*008 that is shed by tumor cells in exosomes. *Cancer Res.* 70: 481–489.
22. Nuckel, H., M. Switala, L. Sellmann, P. A. Horn, J. Durig, U. Duhrsen, R. Kuppers, H. Grosse-Wilde, and V. Rebmann. 2010. The prognostic significance of soluble NKG2D ligands in B-cell chronic lymphocytic leukemia. *Leukemia* 24: 1152–1159.
23. Wu, J. D., L. M. Higgins, A. Steinle, D. Cosman, K. Haugk, and S. R. Plymate. 2004. Prevalent expression of the immunostimulatory MHC class I chain-related molecule is counteracted by shedding in prostate cancer. *J. Clin. Invest.* 114: 560–568.
24. Li, K., M. Mandai, J. Hamanishi, N. Matsumura, A. Suzuki, H. Yagi, K. Yamaguchi, T. Baba, S. Fujii, and I. Konishi. 2009. Clinical significance of the NKG2D ligands, MICA/B and ULBP2 in ovarian cancer: high expression of ULBP2 is an indicator of poor prognosis. *Cancer Immunol. Immunother.* 58: 641–652.
25. Blum, J. S., P. A. Wearsch, and P. Cresswell. 2013. Pathways of antigen processing. *Annu. Rev. Immunol.* 31: 443–473.
26. Grybko, M. J., A. T. Pores-Fernando, G. A. Wurth, and A. Zweifach. 2007. Protein kinase C activity is required for cytotoxic T cell lytic granule exocytosis, but the theta isoform does not play a preferential role. *J. Leukoc. Biol.* 81: 509–519.
27. De Marinis, Y. Z., E. Zhang, S. Amisten, J. Taneera, E. Renström, P. Rorsman, and L. Eliasson. 2010. Enhancement of glucagon secretion in mouse and human pancreatic alpha cells by protein kinase C (PKC) involves intracellular trafficking of PKCα and PKCδ. *Diabetologia* 53: 717–729.
28. Zhao, D., S. Amria, A. Hossain, K. Sundaram, P. Komlosi, M. Nagarkatti, and A. Haque. 2011. Enhancement of HLA class II-restricted CD4$^+$ T cell recognition of human melanoma cells following treatment with bryostatin-1. *Cell. Immunol.* 271: 392–400.
29. Nikodemova, M., J. J. Watters, S. J. Jackson, S. K. Yang, and I. D. Duncan. 2007. Minocycline down-regulates MHC II expression in microglia and macrophages through inhibition of IRF-1 and protein kinase C (PKC)α/βII. *J. Biol. Chem.* 282: 15208–15216.
30. Majewski, M., T. O. Bose, F. C. Sillé, A. M. Pollington, E. Fiebiger, and M. Boes. 2007. Protein kinase C δ stimulates antigen presentation by class II MHC in murine dendritic cells. *Int. Immunol.* 19: 719–732.
31. Bikoff, E. K., R. N. Germain, and E. J. Robertson. 1995. Allelic differences affecting invariant chain dependency of MHC class II subunit assembly. *Immunity* 2: 301–310.
32. Huang, S., S. Gilfillan, S. Kim, B. Thompson, X. Wang, A. J. Sant, D. H. Fremont, O. Lantz, and T. H. Hansen. 2008. MR1 uses an endocytic pathway to activate mucosal-associated invariant T cells. *J. Exp. Med.* 205: 1201–1211.
33. Sloma, I., M. T. Zilber, T. Vasselon, N. Setterblad, M. Cavallari, L. Mori, G. De Libero, D. Charron, N. Mooney, and C. Gelin. 2008. Regulation of CD1a surface expression and antigen presentation by invariant chain and lipid rafts. *J. Immunol.* 180: 980–987.
34. Sillé, F. C., C. Martin, P. Jayaraman, A. Rothchild, G. S. Besra, S. M. Behar, and M. Boes. 2011. Critical role for invariant chain in CD1d-mediated selection and maturation of Vα14-invariant NKT cells. *Immunol. Lett.* 139: 33–41.
35. Brutkiewicz, R. R., C. A. Willard, K. K. Gillett-Heacock, M. R. Pawlak, J. C. Bailey, M. A. Khan, M. Nagala, W. Du, J. Gervay-Hague, and G. J. Renukaradhya. 2007. Protein kinase C δ is a critical regulator of CD1d-mediated antigen presentation. *Eur. J. Immunol.* 37: 2390–2395.
36. Neumann, J., and N. Koch. 2006. A novel domain on HLA-DRβ chain regulates the chaperone role of the invariant chain. *J. Cell Sci.* 119: 4207–4214.
37. Marienhagen, J., A. Dennig, and U. Schwaneberg. 2012. Phosphorothioate-based DNA recombination: an enzyme-free method for the combinatorial assembly of multiple DNA fragments. *Biotechniques* 0: 1–6.
38. Jensen, H., M. Hagemann-Jensen, F. Lauridsen, and S. Skov. 2013. Regulation of NKG2D-ligand cell surface expression by intracellular calcium after HDAC-inhibitor treatment. *Mol. Immunol.* 53: 255–264.
39. Skov, S., M. T. Pedersen, L. Andresen, P. T. Straten, A. Woetmann, and N. Odum. 2005. Cancer cells become susceptible to natural killer cell killing after exposure to histone deacetylase inhibitors due to glycogen synthase kinase-3-dependent expression of MHC class I-related chain A and B. *Cancer Res.* 65: 11136–11145.
40. Chen, Y. C., K. S. Prabhu, A. Das, and A. M. Mastro. 2013. Dietary selenium supplementation modifies breast tumor growth and metastasis. *Int. J. Cancer* 133: 2054–2064.
41. Yan, L., and L. C. DeMars. 2012. Dietary supplementation with methylseleninic acid, but not selenomethionine, reduces spontaneous metastasis of Lewis lung carcinoma in mice. *Int. J. Cancer* 131: 1260–1266.
42. Rock, K. L., S. Gamble, and L. Rothstein. 1990. Presentation of exogenous antigen with class I major histocompatibility complex molecules. *Science* 249: 918–921.
43. Gundimeda, U., J. E. Schiffman, D. Chhabra, J. Wong, A. Wu, and R. Gopalakrishna. 2008. Locally generated methylseleninic acid induces specific inactivation of protein kinase C isoenzymes: relevance to selenium-induced apoptosis in prostate cancer cells. *J. Biol. Chem.* 283: 34519–34531.
44. Kedei, N., D. J. Lundberg, A. Toth, P. Welburn, S. H. Garfield, and P. M. Blumberg. 2004. Characterization of the interaction of ingenol 3-angelate with protein kinase C. *Cancer Res.* 64: 3243–3255.
45. Marinari, U. M., M. Nitti, M. A. Pronzato, and C. Domenicotti. 2003. Role of PKC-dependent pathways in HNE-induced cell protein transport and secretion. *Mol. Aspects Med.* 24: 205–211.
46. Anderson, H. A., D. T. Bergstralh, T. Kawamura, A. Blauvelt, and P. A. Roche. 1999. Phosphorylation of the invariant chain by protein kinase C regulates MHC class II trafficking to antigen-processing compartments. *J. Immunol.* 163: 5435–5443.
47. Robinson, J. W., X. Lou, and L. R. Potter. 2011. The indolocarbazole, Gö6976, inhibits guanylyl cyclase-A and -B. *Br. J. Pharmacol.* 164(2b): 499–506.
48. Gould, C. M., C. E. Antal, G. Reyes, M. T. Kunkel, R. A. Adams, A. Ziyar, T. Riveros, and A. C. Newton. 2011. Active site inhibitors protect protein kinase C from dephosphorylation and stabilize its mature form. *J. Biol. Chem.* 286: 28922–28930.
49. Goodwin, B. J., J. O. Moore, and J. B. Weinberg. 1984. Specific receptors for phorbol diesters on freshly isolated human myeloid and lymphoid leukemia cells: comparable binding characteristics despite different cellular responses. *Blood* 63: 298–304.

50. Zeng, L., S. V. Webster, and P. M. Newton. 2012. The biology of protein kinase C. *Adv. Exp. Med. Biol.* 740: 639–661.
51. Burton, J. D., S. Ely, P. K. Reddy, R. Stein, D. V. Gold, T. M. Cardillo, and D. M. Goldenberg. 2004. CD74 is expressed by multiple myeloma and is a promising target for therapy. *Clin. Cancer Res.* 10: 6606–6611.
52. Suzuki, K. T., Y. Tsuji, Y. Ohta, and N. Suzuki. 2008. Preferential organ distribution of methylselenol source Se-methylselenocysteine relative to methylseleninic acid. *Toxicol. Appl. Pharmacol.* 227: 76–83.
53. Fernández-Messina, L., O. Ashiru, S. Agüera-González, H. T. Reyburn, and M. Valés-Gómez. 2011. The human NKG2D ligand ULBP2 can be expressed at the cell surface with or without a GPI anchor and both forms can activate NK cells. *J. Cell Sci.* 124: 321–327.
54. Qatsha, K. A., C. Rudolph, D. Marmé, C. Schächtele, and W. S. May. 1993. Gö 6976, a selective inhibitor of protein kinase C, is a potent antagonist of human immunodeficiency virus 1 induction from latent/low-level-producing reservoir cells in vitro. *Proc. Natl. Acad. Sci. USA* 90: 4674–4678.